Fluidization of a horizontally driven granular monolayer

Michael Heckel, Achim Sack, Jonathan E. Kollmer, and Thorsten Pöschel

Institut für Multiskalensimulation, Friedrich-Alexander-Universität Erlangen-Nürnberg, Erlangen, Germany

We consider the transition of a horizontally vibrated monodisperse granular monolayer between its condensed state and its three-dimensional gaseous state as a function of the vibration parameters, amplitude, and frequency as well as particle number density. The transition is characterized by an abrupt change of the dynamical state which leaves its fingerprints in several measurable quantities including dissipation rate, sound emission, and a gap size which characterizes the sloshing motion of the material. The transition and its pronounced hysteresis is explained through the energy due to the collective motion of the particles relative to the container.

PACS number(s): 45.70.−n, 46.40.−f

I. INTRODUCTION

Granular material confined in a rectangular container and shaken horizontally under the influence of gravity adopts different dynamical states, depending on the parameters of the oscillation, amplitude, A, and angular frequency, ω.

For deep layers we see essentially two different types of dynamic behavior: for weak forcing (small $\Gamma \equiv A\omega^2$), the granulate adopts a solid state where the particles follow the motion of the container. For more intense forcing, the material near the free surface dilates and performs a sloshing motion while the lower part remains in a dense state characterized by slow convection rolls [1]. For increasing forcing, indicated by a characteristic value $\Gamma_{s \to f}$, there is a sharp transition between the solid state and the fluid state. When the system is in the fluid state, lowering Γ leads to a backward transition which takes place at $\Gamma_{f \to s} < \Gamma_{s \to f}$, that is, there is a pronounced hysteresis [1–3]. This hysteresis can be explained by the fact that for the onset of flow *static* friction between the grains must be overcome, whereas once flowing the grains remain in motion, that is, they interact via *dynamical* friction [1] such that the more dilute case is easier to sustain [2]. The convective flow in deep horizontally shaken systems reveals a complex structure [1,4] and was the subject of intensive research [5–11]. The transition between solid and fluid states was also seen in (quasi) two-dimensional (2D) experiments [12] and simulations [4,12–14] but no hysteresis was found.

The situation is different for a submonolayer of monodisperse spheres subjected to horizontal vibrations, which is addressed in this article. Here we observe two different types of solid-gas transitions depending on the system parameters such as filling fraction, dissipative particle properties, and the parameters of vibration. Even for weak forcing, the particles move with respect to the container except for a narrow range where the driving is too small to overcome rolling friction of the particles. We distinguish three different dynamical states: (*a*) a two-dimensional gaslike state where the particles move incoherently in the entire container by undergoing occasional collisions; (*b*) a state where the particles still move in contact with the floor (that is, in two dimensions) but part of the system is found in a condensed (frequently crystalline) state; and (*c*) a state of high energy which we call a three-dimensional (3D) where the particles experience violent collisions and the system expands in the third dimension.

For the nonhysteretic transition $a \leftrightarrow b$ [15,16], there is no critical value of Γ since the amount of energy transferred from the walls to the particles is unimportant for the dynamical state of the gas [16,17], provided it is large enough to overcome the small resistance due to rolling friction [18]. Instead, the transition can be understood as a kind of resonance effect relating the filling fraction and the amplitude of the vibration [16,19–21]. The mechanism of the transition $a \leftrightarrow b$ resembles the formation of densely packed regions in submonolayer systems driven by a vibrating wall [22], where the dense region appears distant from this wall [23].

While the transition $a \leftrightarrow b$ is well described in the literature, the transition $b \leftrightarrow c$ being the subject of the present article was not described in the literature so far. Obviously, unlike $a \leftrightarrow b$, $b \to c$ must be related to the input of energy to the system as it requires energy to lift the particles to expand in vertical direction and, thus, constitute a 3D system. On the reverse, $c \to b$, when reducing the supply of energy, a 3D gas of particles can transform into a 2D condensate. We will show that the transition $b \leftrightarrow c$ corresponds to an abrupt change of the system's dynamical state. We present a model based on energetic arguments which fully explains the experimental observations, regarding the transition $b \leftrightarrow c$ and its hysteresis in dependence on the parameters of driving, amplitude, and frequency, up to quantitative agreement.

II. SETUP

A polycarbonate box of size $(L_x \times L_y \times L_z) = (97.8 \times 51.4 \times 52.2)$ mm^3 is filled with monodisperse steel balls of diameter, $d = (4.00 \pm 0.02)$ mm, and subjected to horizontal sinusoidal oscillations (see Fig. 1). The box is attached to a strain gauge which in turn is driven by a computer controlled electromechanical actuator, thus, allowing one to measure the force exerted by the actuator onto the box at 10 kHz sample rate. The deviation of the time-dependent box position from the set sinusoidal motion was checked using a Hall-effect based position encoder (resolution 20 μm) and found negligibly small.

Particular attention is payed to the filling of the box: For explanation, we assume the submonolayer being vibrated in horizontal direction at constant frequency, ω, and increasing amplitude, A. For small A, the system is found in the gaslike state a. The transition $a \leftrightarrow b$ takes place independent of frequency, at a certain critical amplitude, $A_{a \leftrightarrow b}$ being a
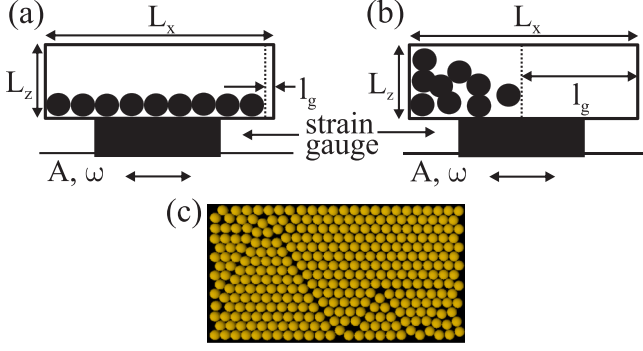
FIG. 1. (Color online) Experimental setup shown for the system in solid state (a) and 3D-gaseous state (b), at the time of reversal of the stroke, when the gap size, l_g, is maximal. A top view of the system in condensed state is shown in (c) (in false colors for better visibility).

decreasing function of the filling rate [21]. The other transition to state c we consider here, is related to the energy of the system, that is (for given ω), the transition depends on A, too. In order to study the transition $b \leftrightarrow c$ we chose the filling rate such that the transition $a \leftrightarrow b$ occurs at a very small value of $A_{a \leftrightarrow b}$, thus, $a \leftrightarrow b$ and $b \leftrightarrow c$ are well separated. Consequently, for all values of A relevant here, the system is *never* in state a but in a (imperfect) crystalline state. Figure 1(c) shows a top view of the system filled with $N = 336$ particles, that is, in condensed state the filling rate is 92.6% of the hexagonal packing such that the particles are loosely packed but the gas state is suppressed.

III. TRANSITION FOR FIXED FREQUENCY OR FIXED AMPLITUDE

Let us first consider the system at fixed frequency, $\omega = 18.85 \text{ s}^{-1} = 3 \text{ Hz} \times 2\pi$, and $A = 1$ mm, where the particles follow synchronously the motion of the box (state b). Increasing the amplitude in steps of 1 mm, at $A_{b \to c} \approx 17$ mm we observe a transition where the hexagonal packing is broken and the granulate extends to the third dimension, thus assuming a gaseous state. After reaching $A_{\max} = 40$ mm, the amplitude is reduced, again in steps of 1 mm and at $A_{c \to b} \approx 9$ mm the system returns back to the condensed state. Performing independent sweeps we found the transition points well reproducible. A pronounced hysteresis was observed, $A_{c \to b} < A_{b \to c}$. For a more quantitative description of the transition, we evaluate the data obtained from the strain gauge to compute the energy dissipation rate,

$$\eta \equiv \frac{\int_T \dot{x}(t) F(t) dt}{4 N m A^2 \omega^2} \qquad (1)$$

by integrating the force between the box and the driver, $F(t)$, obtained from the strain gauge over the period $T = 2\pi/\omega$, where $\dot{x}(t)$ is the velocity of the box. The state-independent normalization factor (see [21]) contains the total mass of the granulate, $Nm = 89.7$ g. For each value of A we recorded data for 22 s. To avoid transient behavior, after switching to a new value of A, we waited for 60 periods before recording data.

Figure 2(a) shows the dissipation rate, η, as a function of the amplitude, A, at constant frequency, $\omega = 18.85 \text{ s}^{-1}$. The
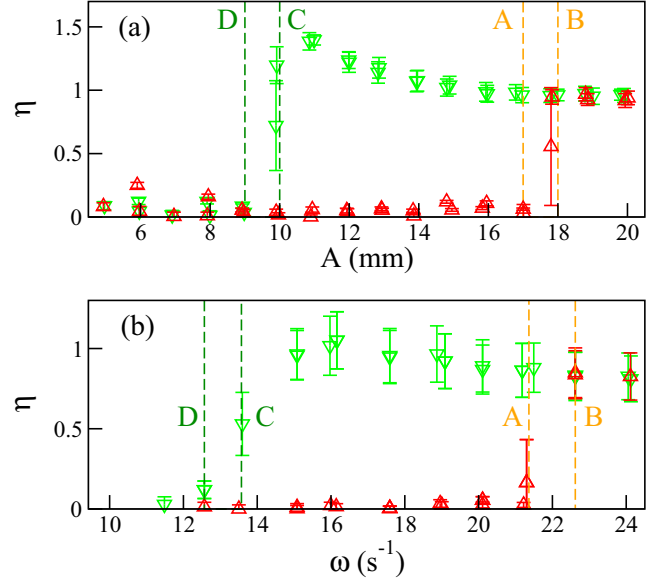

FIG. 2. (Color online) Characterization of the solid-fluid transition, $b \leftrightarrow c$, by means of the dissipation rate, η [see Eq. (1)]. (a) Dissipation rate as a function of amplitude, $\eta(A)$, for fixed frequency, $\omega = 18.85 \text{ s}^{-1}$. (b) Dissipation rate as a function of frequency, $\eta(\omega)$, for fixed amplitude, $A = 15$ mm. Error bars show the standard deviation of independent measurements. Red triangle up symbols indicate increasing amplitude ($b \to c$); green triangle down symbols stand for decreasing amplitude ($c \to b$). Vertical dashed lines labeled A–D correspond to the labels shown in Fig. 3.

error bars show the variance over the 22 s of measurement. Sharp jumps characterize the hysteretic transition. When in solid state, the material behaves essentially like a passive additional mass attached to the box which does not significantly contribute to the total dissipation of the system, thus $\eta \gtrsim 0$. In contrast, in fluidized state the particles undergo violent dissipative collisions with one another and with the container walls. The lost mechanical energy is resupplied to the system by the driver and measurable via Eq. (1) using the exerted force, $F(t)$. Note that the characteristic dependence of the energy dissipation rate on the dynamic state of the granulate was shown before for the gas-solid transition in the absence of gravity and can be fully understood for this case [19–21].

Complementary to $\eta(A)$, Fig. 2(b) shows the dissipation rate as a function of frequency, $\eta(\omega)$ for fixed amplitude, $A = 15$ mm, showing similar characteristics regarding the transition and the hysteresis.

IV. CHARACTERIZATION IN FULL PARAMETER SPACE

So far, we considered the transition for a particular frequency, $\omega = 2\pi \times 3$ Hz or for fixed amplitude, $A = 15$ mm, showing that the transition $b \leftrightarrow c$ depends on both parameters of driving, A and ω, which is consistent with argument given above indicating that the transition is related to energy. This is different from the transition $a \leftrightarrow b$ which is independent of frequency [21]. Figure 3 characterizes the transition $b \leftrightarrow c$ and its hysteresis for the full space of parameters. To obtain the figure, for each value of ω we swept $A = (1, 2, 3, \ldots, 40)$ mm where each amplitude was kept constant for 60 s. Red symbols
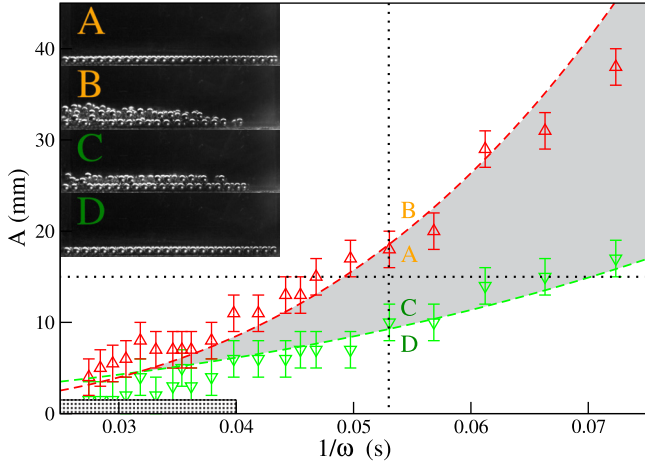
FIG. 3. (Color online) The transition $b \to c$ (red, triangle up) and $c \to b$ (green, triangle down) in parameter space (A, ω). The dashed lines are the solution of our model and indicate that both transitions take place at critical values of the kinetic energy. The range of hysteretic behavior appears gray shaded. The vertical dotted line marks $\omega = 2\pi \times 3$ Hz corresponding to Fig. 2(a). For this frequency, the insets show snapshots at the end of the left stroke close to the transition amplitudes marked A–D here and in Fig. 2: A, condensed metastable state; B, stable fluidized state; C, metastable fluidized state; D, stable condensed state. The horizontal dotted line marks the particular value, $A = 15$ mm, used in Fig. 2(b). For A and $1/\omega$ both small (marked region), where $A \sim l_g$, the transitions $a \leftrightarrow b$ and $b \leftrightarrow c$ interfere.

mark $A_{b \to c}$ indicated by the energy dissipation criterion [see Fig. 2(b)]. Subsequently, the amplitude was swept again, $A = (40, 39, \ldots, 1)$ mm, and the transition point, $A_{c \to b}$, is shown by green symbols. The particular values of A and ω used for Fig. 2 are shown by dotted lines.

The transition $b \leftrightarrow c$ leaves its fingerprints in at least two more measurable quantities, namely, in the sound emission and the *gap size*, l_g, which was introduced in [6] to describe the dynamical state of a horizontally shaken granulate. The characterization of the transition by means of these values as functions of amplitude and frequency agrees almost perfectly with the analysis based on the dissipation rate, η, and will be discussed elsewhere.

V. MODEL

A necessary condition for the solid-fluid transition is that particles gain enough energy to leave the monolayer, such that the granulate can expand in vertical direction. Let us consider the coherent motion of the monolayer in the sinusoidally vibrated container, $x(t_c) = A \sin(\omega t_c)$ [24]. The extension of this block is $L_x - l_g^s$ where $l_g^s \approx 0.8$ mm is the gap size in the solid state [see Fig. 1(c)]. The block leaves the wall at the inward stroke at time $t = 0$ when the velocity is maximal, $|v| = A\omega$. From equating the time-dependent positions of the wall and the block, we obtain the time, t_c, of the collision with the opposite wall:

$$\omega t_c = \sin(\omega t_c) + l_g / A. \tag{2}$$

We expand this expression to third order around $\omega t_c = 0$, solve for ωt_c, and insert into $\dot{x} = A\omega \cos(\omega t)$ to obtain the relative velocity between the container wall and the block at the time when the impact takes place,

$$\Delta v = A\omega (1 - \cos[(6l_g/A)^{1/3}]), \tag{3}$$

which evaluates to $\Delta v \approx 0.066$ m/s for $A = A_{b \to c} \approx 17$ mm, $\omega = 18.85$ s^{-1}, and $l_g \approx 0.8$ mm. As can be seen in Fig. 1(c), the system forms straight rows consisting of 24 particles each. If all spheres in such a row are pushing like a single particle of greater mass against the wall their combined energy allows one to eventually lift one particle. In this way, if all $N_x = 24$ particles fitting in one row in the direction of shaking would coherently collide with the wall, the necessary velocity to lift a single particle by its diameter is $\sqrt{2gd/N_x} \approx 0.06$ m/s, that is, the energetic argument explains the transition at $A_{b \to c} \approx 17$ mm, observed in the experiment. When the first particles leave the lowest layer, the gap size increases and, consequently, Δv increases rapidly (e.g., $\Delta v \approx 0.12$ m/s for $l_g = 2$ mm) and more particles become airborne, eventually leading to a burstlike fluidization transition. Note that the increase of the necessary velocity due to the reduction of N_x is small as compared to the increase of Δv given by Eq. (3) due to the increase of the gap size, l_g, when a particle becomes airborne.

To obtain a lower estimate for $A_{c \to b}$ when lowering the amplitude, coming from a fluidized state, we compare the kinetic energy of the collision at maximum possible relative velocity, $2A\omega$, with the energy needed to lift a particle by its diameter. The estimate, $A_{c \to b} > \omega^{-1} \sqrt{gd/2} \approx 7.4$ mm for the lower limit agrees with the experimental value, $A_{c \to b} \approx 9$ mm. Thus, the energetic argument explains the hysteresis, and provides a good estimate for $A_{b \to c}$ and a valid lower limit for $A_{c \to b}$. As further indication for the energy argument to explain the hysteresis, in Fig. 4 we show $\eta(A)$, similar as in Fig. 2(a) but for lower particle number density, that is, for 224 particles forming a $\frac{2}{3}$ submonolayer. Because of the larger initial gap size, l_g, following the discussion above, we expect a fluidization at smaller $A_{b \to c}$ and the mechanism leading to a burstlike transition suppressed, being the reason for the hysteresis of the transition $b \leftrightarrow c$. Indeed, for a submonolayer, the transition occurs gradually and the hysteresis is suppressed.
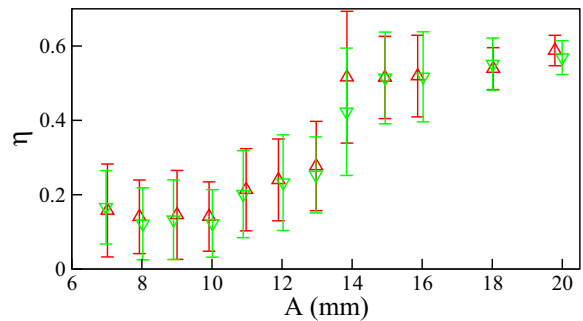

FIG. 4. (Color online) Energy dissipation rate of a $\frac{2}{3}$ submonolayer. All other parameters as for Fig. 2. In agreement with the energy argument for the explanation of the hysteresis, here the transition $b \leftrightarrow c$ occurs gradually (no bursts). Consequently, no hysteresis is found.

VI. CONCLUSION

When a granular (sub-)monolayer is subjected to horizontal vibrations, three different states are observed, depending on the parameters of driving. While the transition between the 2D gas state and the condensed state, occurring at a critical amplitude but independently of frequency, is well described in the literature, here we discuss the transition between the condensed state and a 3D gas state: For fixed frequency, by slowly varying the amplitude of the oscillation, we observe an abrupt change of the system's dynamical state where the system expands to the vertical dimension. We find a well defined hysteresis of the transition which can be explained by considering the energy of the collective motion of the particles relative to the container. Looking to the full parameter space, (A, ω), we find both transitions forward and backward on lines where $A \sim \omega^{-1}$

also indicating that the transitions occur at critical energies. We present a corresponding model description, based on energetic arguments, which describes both the transition and its hysteresis up to good quantitative agreement with the experimental results. Reducing the particle number density to a $\frac{2}{3}$ submonolayer, the transition occurs gradually and the hysteresis vanishes, which is also in agreement with the model description.

[1] S. G. K. Tennakoon, L. Kondic, and R. P. Behringer, Europhys. Lett. **45**, 470 (1999).

[2] G. Metcalfe, S. G. K. Tennakoon, L. Kondic, D. G. Schaeffer, and R. P. Behringer, Phys. Rev. E **65**, 031302 (2002).

[3] S. Aumaitre, C. Puls, J. N. McElwaine, and J. P. Gollub, Phys. Rev. E **75**, 061307 (2007).

[4] K. Liffman, G. Metcalfe, and P. Cleary, Phys. Rev. Lett. **79**, 4574 (1997).

[5] M. Medved, D. Dawson, H. M. Jäger, and S. R. Nagel, Chaos **9**, 691 (1999).

[6] M. Medved, Phys. Rev. E **65**, 021305 (2002).

[7] S. S. Hsiau, M. Y. Ou, and C. H. Tai, Adv. Powder Technol. **13**, 167 (2002).

[8] A. Raihane, O. Bonnefoy, J.-L. Gelet, J.-M. Chaix, and G. Thomas, Powder Technol. **190**, 252 (2009).

[9] A. Raihane, O. Bonnefoy, S. Nadler, J.-L. Gelet, J.-M. Chaix, and G. Thomas, *Convective Flow in a Horizontally Vibrated 3D Granular Packing*, AIP Conf. Proc. No. 1145 (AIP, Melville, NY, 2009), p. 721.

[10] S. Nadler, D. Bonnefoy, J.-M. Chaix, G. Thomas, and J. L. Gelet, Eur. Phys. J. E **34**, 66 (2011).

[11] T. Pöschel, D. E. Rosenkranz, and J. A. C. Gallas, Phys. Rev. E **85**, 031307 (2012).

[12] G. H. Ristow, G. Straßburger, and I. Rehberg, Phys. Rev. Lett. **79**, 833 (1997).

[13] J. A. C. Gallas, H. Herrmann, and S. Sokołowski, J. Phys. II **2**, 1389 (1992).

[14] C. Salueña, T. Pöschel, and S. E. Esipov, Phys. Rev. E **59**, 4422 (1999).

[15] G. Straßburger, A. Betat, M. A. Scherer, and I. Rehberg, in *Workshop on Traffic and Granular Flow*, edited by D. E. Wolf, M. Schreckenberg, and A. Bachem (World Scientific, Singapore, 1995), pp. 329–334.

[16] F. F. Chung, S.-S. Liaw, and M. C. Ho, Granular Matter **12**, 369 (2010).

[17] G. Straßburger and I. Rehberg, Phys. Rev. E **62**, 2517 (2000).

[18] For very low driving, when the rolling friction cannot be neglected as compared to sliding, self-organized stripelike patterns may appear [15, 25, 26].

[19] M. N. Bannerman, J. E. Kollmer, A. Sack, M. Heckel, P. Mueller, and T. Pöschel, Phys. Rev. E **84**, 011301 (2011).

[20] J. E. Kollmer, A. Sack, M. Heckel, and T. Pöschel, New J. Phys. **15**, 093023 (2013).

[21] A. Sack, M. Heckel, J. E. Kollmer, F. Zimber, and T. Pöschel, Phys. Rev. Lett. **111**, 018001 (2013).

[22] A. Kudrolli, M. Wolpert, and J. P. Gollub, Phys. Rev. Lett. **78**, 1383 (1997).

[23] There is a large body of literature on gas-solid transitions in driven and undriven systems, including coexistence of gaseous and solid phases. For an extended overview see [27], and references therein.

[24] B. Drossel and T. Prellberg, Eur. Phys. J. B **1**, 533 (1998).

[25] D. Krengel, S. Strobl, A. Sack, M. Heckel, and T. Pöschel, Granular Matter **15**, 377 (2013).

[26] S. Mobarakabadi, E. N. Oskoee, M. Schröter, and M. Habibi, Phys. Rev. E **88**, 042201 (2013).

[27] I. S. Aranson and L. S. Tsimring, Rev. Mod. Phys. **78**, 641 (2006).